Toxicologic Pathology, 34:111–117, 2006

ISSN: 0192-6233 print / 1533-1601 online
DOI: 10.1080/01926230500404126

Imaging Methods for Morphological and Functional Phenotyping of the Rodent Heart

CRISTIAN T. BADEA,[1] ELIZABETH BUCHOLZ,[1] LAURENCE W. HEDLUND,[1] HOWARD A. ROCKMAN,[2] AND G. ALLAN JOHNSON[1]

[1]*Center for In Vivo Microscopy, Duke University Medical Center, Durham, North Carolina 27710, USA*
[2]*Division of Cardiology, Duke University Medical Center, Durham, North Carolina 27710, USA*

ABSTRACT

Small animal imaging has a critical role in phenotyping, drug discovery, and in providing a basic understanding of mechanisms of disease. Translating imaging methods from humans to small animals is not an easy task. The purpose of this work is to compare two cardiac imaging modalities, i.e., magnetic resonance microscopy (MRM) and microcomputed tomography (CT) for preclinical studies on rodents. We present the two technologies, the parameters that they can measure, the types of alterations that they can detect, and show how these imaging methods compare to techniques available in clinical medicine. While this paper does not refer per se to the cardiac risk assessment for drug or chemical development, we hope that the information will effectively address how MRM and micro-CT might be exploited to measure biomarkers critical for safety assessment.

Keywords. Cardiac imaging; micro-CT; magnetic resonance microscopy; mouse.

INTRODUCTION

Transgenic manipulations in mice and rats are increasingly used to probe genetic and physiological aspects of human cardiovascular physiology. Cardiac studies in small animals are not easy. The extremely small size (∼0.1 g and 7 mm long axis) and extremely fast rates (∼600 beats/min) of murine hearts under physiological conditions have made in vivo studies of murine cardiac metabolism, function, and morphology difficult. In vivo open chest models of transgenic mouse cardiac function were among the first attempts to characterize the dynamic role of the heart in the cardiovascular system, but with the disadvantages that these procedures are invasive in nature and the subject does not survive the analysis precluding longitudinal studies (James et al., 1998). Noninvasive in vivo imaging appears to be the ideal solution. Whereas clinical imaging modalities provide accurate assessment of the human heart, their extension from humans to rodents presents several formidable scaling challenges. For example, acquiring CT and MR images of the mouse heart with organ definition and fluidity of contraction comparable to that which can be achieved in humans requires an increase by a factor of about 3000 in spatial resolution and a 10-fold increase in temporal resolution. Therefore, high spatial and temporal resolutions are fundamental requirements for murine cardiac imaging.

Several imaging techniques are being adapted for mouse studies, including x-ray computed tomography (CT), positron emission tomography (PET), echocardiography, and magnetic resonance imaging (MRI). Among the imaging methods, ultrasound echocardiography is presently the most commonly used technology for cardiovascular mouse imaging, and its applications are expanding. M Mode and Doppler echocardiography have been used extensively to phenotype the cardiovascular system in a variety of genetic mouse models (Hoit, 2001). More recently, 2D and 3D echocardiography in mice have emerged (Dawson et al., 2004). Although echocardiography is the method of choice to estimate cardiac function, this method still uses some model-based estimation that relies on geometric assumptions that work well only in normal hearts (Hoit and Walsh, 2001; Camici, 2003).

This paper focuses on two additional imaging methods—magnetic resonance microscopy (MRM) and micro-CT. Unlike echocardiography, the fundamental tomographic nature of MRI and CT eliminates the need for geometric assumptions when calculating ventricular volume, mass, and function. MR microscopy has been applied to assess both cardiac morphology and function in rodents (Franco et al., 1998; Ruff et al., 1998; Slawson et al., 1998; Wiesmann et al., 2000; Brau et al., 2004). We recently proposed a micro-CT based method appropriate for in vivo characterization of cardiac structure and function in mice (Badea et al., 2005), where true 4D datasets are collected with an isotropic spatial resolution of 100 microns and a temporal resolution of 10 ms during the cardiac cycle.

This work compares MR microscopy and micro-CT with an overview of the challenges posed by these two technologies for studies on rodents compared to clinical medicine, what each method can measure, and the ability of each method to detect types of alterations. Although this paper does not specifically refer to the cardiac risk assessment for drug or chemical development, we hope that the information will effectively address how MRM and micro-CT might be exploited to measure biomarkers critical for safety assessment.

Address correspondence to: Cristian T. Badea, Box 3302, Duke University Medical Center, Durham, NC 27710, USA; e-mail: chris@orion.duhs.duke.edu

Abbreviations: 2D, 2-dimensional; 3D, 3-dimensional; 4D, 4-dimensional; CT, computed tomography; LV, left ventricle; MI, myocardial infarction; MR, magnetic resonance; MRM, magnetic resonance microscopy; PET, positron emission tomography; rf, radio frequency; SNR, signal-to-noise ratio; SSFP, steady state free precession.

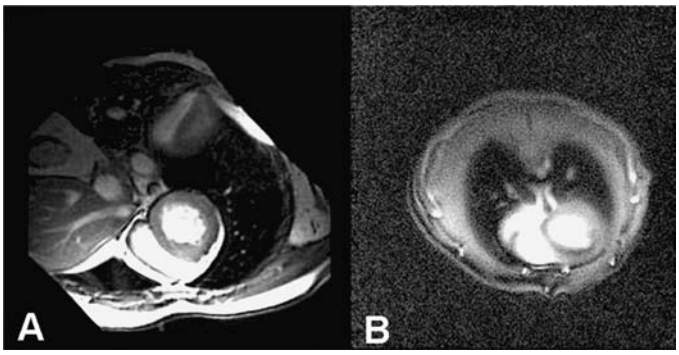

FIGURE 1.—Comparison of (a) a cardiac gated human MRI and (b) a cardiac gated MR microscopy image of a mouse. The slice in a) is 5 mm with in plane resolution of 1 × 1 mm. The slice in (b) is 1.0 mm with in plane resolution of 0.2 × 0.2 mm.

Cardiac Magnetic Resonance Microscopy

One of the most significant challenges of magnetic resonance microscopy is a much weaker signal than is routinely available in clinical imaging. The brightness in each picture element (pixel) represents the signal from a small volume of tissue, i.e., a voxel of the specimen. A typical clinical cardiac image (Figure 1a) represents a 5 mm thick slice of the heart with in plane resolution of 1 × 1 mm, (voxels of 5 mm^3). Table 1 shows recent work in both the rat and mouse. Brau et al. (2000) report three-dimensional images in the rat heart with a resolution of 0.175 × 0.175 × 1.0 mm^3, i.e., a reduction of nearly 140×. Wiesmann et al. (2003) have reported resolution of 0.049 × 0.098 × 0.30 mm in the mouse (voxels of 0.00144 mm^3). Thus, the signal in the highest resolution MR images of the mouse is inherently at least 1000× weaker than that in the clinical arena. Since the signal from a voxel increases with higher field, the majority of work on mouse models is undertaken at higher magnetic fields ranging between 4T and 11.75 T. Unfortunately increased magnet strength carries with it increased engineering and technical challenges.

The signal for each pixel is encoded through the use of a magnetic field gradient. While a thorough discussion of the encoding process is beyond the scope of this article, a complete discussion of MRI is available in reference (Haacke et al., 1999). The most critical issue about spatial encoding is the strength of these gradients. The gradient coils in a clinical scanner typically achieve strengths of 50 mT/m compared to the gradients required for imaging a rat or mouse that can exceed 700 mT/m. The construction of specialized radiofrequency coils to capture the weak signal pose additional technical challenges.

MRM and micro-CT share a critical challenge to stabilize and synchronize the ventilatory and cardiac motion to the pulse sequence used to generate the image. In the clinical arena for cardiac imaging, patients are instructed to hold their breath for typically 15–30 seconds. The weak signals in the mouse and rat require encoding for both CT and MR over a much longer time span, typically many respiratory and cardiac cycles. Unless the acquisition is carefully synchronized so each pulse of the sequence is executed with the anatomy in the same position, there will be substantial image blur and artifact. Ventilatory synchronization was first suggested by Hedlund et al. (1986). Animals are intubated to synchronize breathing with the image acquisition so that each element of the image is captured at the same point in the ventilatory cycle (Hedlund and Johnson, 2002). A problem arises in MRI, where one must synchronize the radio frequency (rf) pulses used to excite the tissue to both the ventilatory and cardiac cycle while keeping the pulse timing very regular. Figure 2a shows an image of a live rat with respiratory and cardiac gating using the (Cartesian) encoding method used most routinely in clinical scanners.

Even with the careful synchronization, there are significant "phase ghosting" artifacts that arise from motion and subtle variation in the timing between the rf pulses used to generate the MR signal. Note for example in Figure 2a the poorly defined boundary on the right ventricle. Also note the absence of signal (flow void artifact) in the vena cava (arrow 1). The MR signal is extremely sensitive to motion, in this case the motion of the blood in the cardiac chambers and vessels. Finally, note the artifact at the edge of the right lung (arrow 2). This artifact, which looks suspiciously like a tumor, is in fact a signal arising from the regular pulsation in the vena cava. The pulsation frequency is just right in this

TABLE 1.—Recent rodent cardiac imaging references show voxels ranging from 0.228 mm^3 to 0.00144 mm^3 with the highest resolution work done nearly 3,500 times smaller than routine clinical exams.

Reference	Rat/Mouse	Slice (mm)	Resolution (mm)	Voxel (mm^3)
(Al-Shafei et al., 2002)	Rat	1.5	0.390 × 0.390	0.228
(Barone et al., 2001)	Rat	1	0.312 × 0.312	0.097
(Nahrendorf et al., 2003)	Rat	1	0.230 × 0.230	0.069
(Brau et al., 2004)	Rat	1	0.175 × 0.175	0.031
(Zhou et al., 2003)	Mouse	1	0.234 × 0.234	0.0547
(Berr et al., 2005)	Mouse	1	0.2 × 0.2	0.04
(Ruff et al., 2000)	Mouse	0.2	0.10 × 0.10	0.002
(Itskovich et al., 2003)	Mouse	0.3	0.078 × 0.078	0.00182
(Wiesmann et al., 2003)	Mouse	0.3	0.049 × 0.098	0.00144

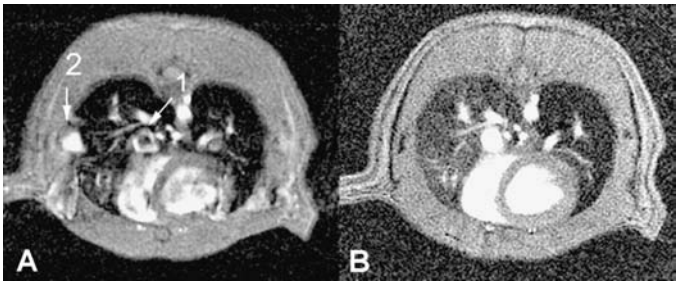

FIGURE 2.—Cardiac gated, scan synchronous gated MR images of the rat have been acquired with (a) traditional Cartesian encoding methods and (b) projection encoding. Even with careful synchronization, there are significant "phase ghosting" artifacts arising from motion and subtle variation in the timing between the rf pulses used to generate the MR signal. Note for example in (a) the poorly defined boundary on the right ventricle. Note the absence of signal (flow void artifact) in the vena cava (arrow 1). The MR signal is extremely sensitive to motion, in this case the motion of the blood in the cardiac chambers and vessels. Finally, note the artifact at the edge of the right lung (arrow 2). Reprinted with permission from (Brau et al., 2004).

example to result in an accumulation of signal displaced horizontally from the source (the vena cava). Glover and Pelc (1988) suggested the use of a projection encoding method that is much more immune to these motion artifacts. Gewalt et al. were the first to apply projection encoding to the special needs of cardiopulmonary imaging in the rat (Gewalt et al., 1993). More recently, Brau et al. (2004) have refined this approach to support dynamic cardiac studies. Figure 2b from (Brau et al., 2004) shows a projection encoded image of the same animal imaged in Figure 2a. The method provides an extra degree of immunity from the very rapid cardiac and respiratory motion encountered in the rat and variations in signal from variation in the R-R interval.

A strength of MRI is image contrast, i.e., the ability to distinguish one tissue from another. The MR signal is generated by a series of radio frequency pulses used to excite the tissues and generate the signal, separated by an interval (TR) that allows for recovery of the tissue from the previous excitation. A wide range of signal manipulations is possible in MRI by using sophisticated spin preparation techniques to produce images where the blood is black or images in which the blood is white (Berr et al., 2005). For simple 2-dimensional imaging, the blood appears brighter than the myocardium since fresh (unexcited) blood flows into the imaging slice between the excitations. One can exploit this fact with a series of rapid pulses separated by TR$\sim$5–10 ms that results in signals from the heart at up to 20 different time points in the cardiac cycle. The process can be repeated for multiple cycles of the heart. Since the R-R interval in the mouse is $\sim$100 ms, one can, in principle, generate sufficient data for images covering the entire cardiac cycle in $\sim$25 seconds with in plane resolution of $\sim$150 microns. Unfortunately the very weak signal from the small voxels in the rodent requires averaging much more in order to get sufficient signal for good anatomic definition.

Figure 3 shows work currently under way in our laboratory to capture the weak signal in as effective a fashion as possible using "steady-state" methods (Scheffler and Lehnhardt, 2003). Images were generated at 7T using steady-state free precession (SSFP) 2D projection encoding (Brau et al., 2004) in conjunction with ventilatory and cardiac synchronization. The total acquisition time was 20 minutes with in plane resolution of $\sim$200 microns in 1 mm thick slices. Note in particular the bright signal from the blood in the chambers and in all the pulmonary vasculature. There is very little signal in the lung, since there are very few protons in the parenchyma.

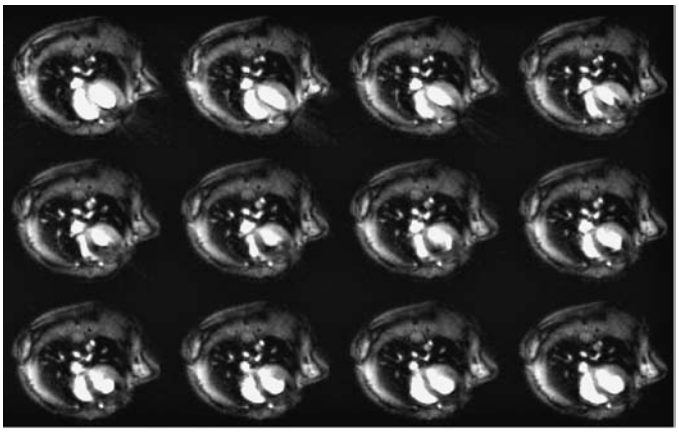

FIGURE 3.—MR images of a live mouse acquired with projection encoding through 12 points in the cardiac cycle. The images were generated at 7.0 T using an SSFP projection encoding method with cardiac gating and scan synchronous ventilation. Slice thickness is 1 mm with in-plane resolution of $\sim$200 microns. Total scan time was 20 minutes.

Cardiac Micro-CT

Micro-CT has been used to image the isolated, fixed rodent heart with 25 micron spatial resolution (Jorgensen et al., 1998) resulting in a 3D reconstruction of the heart with superb anatomical detail. However, in vivo cardiac micro-CT in mice was considered to be "illusive" (Lazebnik and Wilson, 2001) or "impossible with the state of the art technology" (Yea et al., 2004). Micro-CT and MRM share the same challenges of cardiac and ventilatory motion. The analogous problem to the limited signal (in MRM) arises from the relationship between the number of x-rays used to generate the CT image (dose) and the spatial resolution. As one reduces the size of the voxel, the dose must increase simultaneously to maintain the signal to noise in the image (Ford et al., 2003). We have developed a prototype cone beam micro-CT system with a design that addresses two of the most significant barriers to micro-CT in small animals—the reduced signal-to-noise imposed by the smaller voxels and motion (Badea et al., 2004a; Badea 2004b). The most direct approach to increasing the signal-to-noise ratio (SNR) is to increase the total fluence rate. It is not possible to significantly increase the fluence rate in most of the laboratory and commercial micro-CT systems currently in use (Paulus et al., 2000, 2001; Wang and Vannier, 2001), since these systems use smaller fixed focal spot x-ray tubes. One can integrate over extended periods with these devices, but then biological motion poses the resolution limit. Our system allows the use of high x-ray photon fluence tubes that are 250 times brighter than the tubes on commercial micro-CT systems. Moreover the system takes advantage of integrated physiologic monitoring and control of breathing and cardiac motion that has been developed previously for MR imaging of small animals (Hedlund and Johnson, 2002) to limit artifacts and motion blur from both respiratory and cardiac motion.

Another major challenge for in vivo micro-CT is the low soft tissue contrast resolution compared with that in MR. Micro-CT scanning time for a complete 3D dataset is on the order of 10 minutes with most of the systems available. Radiographic contrast agents used in the clinical arena produce contrast in the vascular by providing high x-ray absorbing iodine atoms. Unfortunately, traditional radiographic contrast agents are cleared by the kidneys in $\sim$10–30 seconds. Fortunately, a new class of blood pool contrast agent for CT (Weichert et al., 1998; Vera and Mattrey, 2002) with prolonged vascular residence time is now available for small animal imaging—Fenestra VC (Alerion Biomedical, Inc., San Diego, CA).

The micro-CT system we have developed acquires projected radiographs of the animal as the animal is rotated in front of a high-resolution x-ray detector. These projection images are then used to reconstruct a 3D image array ($1024 \times 1024 \times 1024$) from which one can display slices in any plane with resolution of $100 \times 100 \times 100$ microns. Isotropic (3D) volume images of the mouse heart have been acquired at

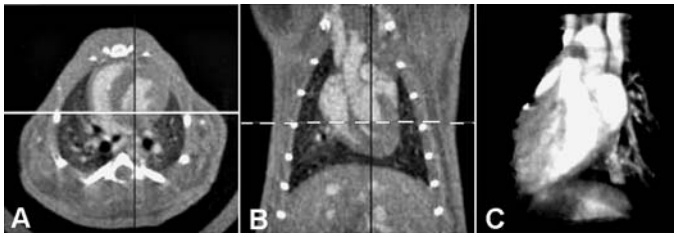

FIGURE 4.—Representative images extracted from a 4D micro-CT image of a live C57/BL6 mouse. These images are all derived from a single 3D volume at end diastole. The continuous white line in the transverse image (a) show the plane for the coronal image (b). Since the blood pool has been highlighted via the contrast agent, it is possible to render a 3-dimensional image of the chambers of the heart (c).

multiple points of the cardiac cycle with a temporal resolution of 10 ms. The resulting 4D images (3D volume images at multiple time points in the R-R cycle) can provide accurate volume and wall motion measurements along any arbitrary plane throughout the cardiac cycle. The high x-ray attenuation of the blood- pool contrast agent produces excellent contrast ~500 HU difference between blood and muscle facilitating quantitative measure of ejection fraction and cardiac output.

Figure 4 shows representative images from a single time point in the cardiac cycle of a C57BL/6 mouse. The isotropic nature of the image is demonstrated in Figure 4a and b. Chambers of the heart are clearly outlined because of the difference in x-ray attenuation produced by the blood pool agent. The transverse slice shown in Figure 4a is only 100 microns thick with 100 × 100 micron in plane resolution. The data can be resliced along the white line in Figure 4a yielding the coronal view seen in Figure 4b. Figure 4c shows a volume rendered image of the data demonstrating the potential for very accurate measurement of chamber volumes. Since the data are isotropic, one can reslice along any arbitrary axis without loss of spatial resolution. For example, Figure 5 shows an oblique plane parallel to the aorta that clearly identifies the aortic valve (arrow).

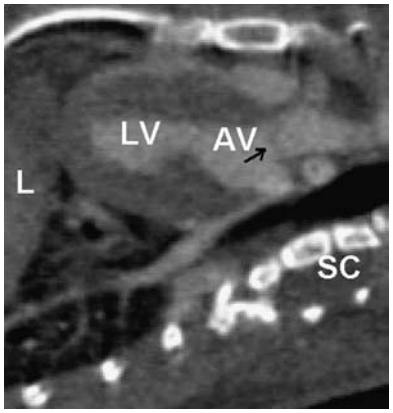

FIGURE 5.—The isotropic resolution in micro-CT allows one to reslice along any arbitrary plane without loss of resolution. In this example, the oblique sagittal plane demonstrates the aortic valve (AV) (arrow). A number of anatomical features are indicated including left ventricle (LV), liver (L), and spinal cord (SC).

TABLE 2.—A comparison of cardiac measures for 2 MI mice vs. the controls C57BL/6.

Cardiac parameter	MI-1	MI-2	C57BL/6 (n = 5)
LV diastolic vol (μl)	73.05	34.61	49 ± 10.7
LV systolic vol (μl)	51.95	18.43	24 ± 3.8
Heart rate (beats/min)	476	638	507 ± 20.91
Ejection fraction (%)	28.88 %	46%	50.9 ± 2.81
Stroke volume (μl)	21.10	16.18	25 ± 6.3
Cardiac output (ml /min)	9.74	10.3	12.62 ± 2.0

To show the potential of micro-CT in murine cardiac imaging, we present here the evaluation of cardiac anatomy and function in a model for myocardial infarction (MI) obtained by left coronary artery ligation in two C57BL/6 mice. Both MI and control animals were injected with a blood pool contrast agent (Fenestra VC) and scanned using our micro-CT system. For each animal, we acquired datasets corresponding to a time resolution of 10 ms in the cardiac cycle. MI mice showed significant morphological changes such as heart wall thinning and differences in cardiac dynamics when compared to the controls (C57BL/6). On the other hand, left ventricle (LV) systolic and diastolic volumes and the cardiac parameters based on the LV measurement, i.e., ejection fraction, stroke volume and cardiac output showed notable differences compared to the controls (see Table 2). Figure 6a shows the unusual thinning of the LV close to the apex of the heart (yellow arrow). The tissue in that region was observed to look different during dissection and was necrotic (Figure 6b).

DISCUSSION

MRM and micro-CT share several common challenges. Both imaging methods require scan times that are much longer than a single respiratory or cardiac cycle. Real time imaging, which is common in ultrasound, is not possible with the current state-of-the-art. Thus, management of physiologic motion is absolutely essential. Our approach for both MRM and micro-CT uses active control of the ventilation with cardiac triggers for the RF pulsing (MRM) or x-ray exposure (micro-CT). At present, this approach requires intubation of the animal, which in turn requires skilled technicians and some setup time. Therefore, neither method can be thought of as a high throughput screening methodology.

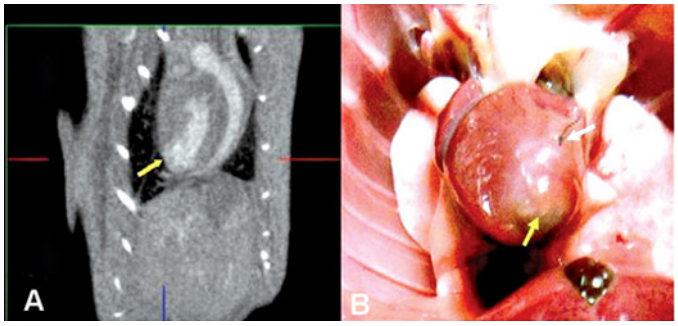

FIGURE 6.—Micro-CT images show the unusual thinning of the left ventricle (yellow arrow) in a model for myocardial infarction (MI) obtained by left coronary artery ligation (white arrow) in C57BL/6 mice. At dissection the tissue close to the apex of the heart was observed to look different and was necrotic (b).

Both methods require a fair degree of sophistication to interpret images. The images are reconstructed from physical measurements. For MR, the measurements are of magnetic properties of the tissues. For CT, the measurements are transmitted radiation—simply a series of radiographs at multiple angles. Both methods require consistent data, i.e., that the anatomy be in the same place for each of the many measurements required. When motion, flow effects, and the presence of contrast agent vary from measurement to measurement, artifacts in the image can be misinterpreted as anatomic or pathologic variation. Without a solid understanding of the underlying imaging principles, misleading interpretations of images can occur, as shown by Figure 2.

Figures 7 and 8 show a side-by-side comparison of a C57 BL/6 mouse imaged with MR microscopy at 7 T with micro-CT using the blood pool contrast agent. The MR images are 1 mm thick 2D images at 12 time points in the R-R interval. The micro-CT images, also acquired at 12 points in the cardiac cycle, are representative 0.1 mm thick coronal slices, each extracted from the 3D volume at that point in the R-R interval. Contrast is more easily interpreted in micro-CT since the tissue differentiation is based entirely in the x-ray attenuation. Air in the lung does not attenuate the signal appreciably, so the reconstruction algorithm registers lung as black. Muscle attenuates the x-rays more. Bone and the blood pool agent with the high absorbing iodine provide the highest attenuation that makes the brightest signal in the image. The inherent contrast between blood and myocardium is limited. The contrast between pulmonary vasculature and air in the lung is good, which allows excellent definition of the pulmonary architecture.

Contrast in MR is much more complicated depending on the rapidity of the pulses, the types of pulses, delay times after the pulses, flow properties, and MR properties of the tissues. Note in Figure 7 the changes in signal through the cardiac cycle. At diastole, where the blood is relatively stationary, there is strong signal everywhere. As the heart contracts, blood accelerates and flow effects alter the signal. For example, note the swirling pattern at the top of the aortic arch in Figure 7a–7c. In 7h–l, the blood is moving so rapidly that there is a dark hole in the left ventricle as the heart contracts rapidly toward systole. The lung has very little signal because of the limited number of protons, and the magnetic properties of lung are such that any MR signal from lung parenchyma or vasculature will decay very rapidly (Durney et al., 1996). The strength of MR lies in the much higher degree of flexibility in how contrast can be manipulated. For example, flow can be measured quantitatively. Again, the weakness in MR is that interpretation requires understanding of the underlying principles of the imaging method.

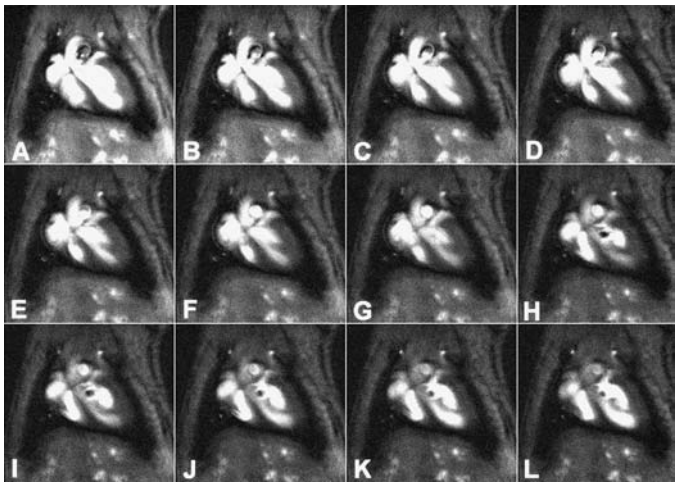

FIGURE 7.—MR images in coronal orientation of a live mouse acquired with projection encoding through 12 points in the cardiac cycle. The images were generated at 7.0 T using an SSFP projection encoding method with cardiac gating and scan synchronous ventilation. Slice thickness is 1 mm with in plane resolution of ~200 microns.

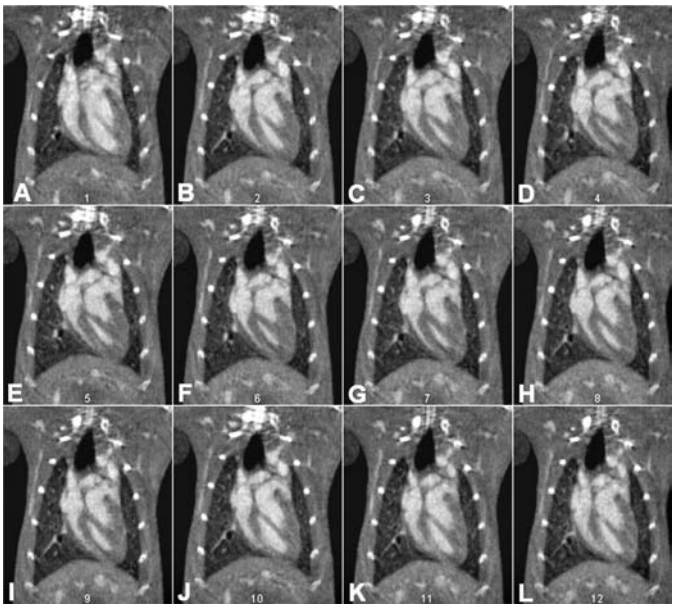

FIGURE 8.—Micro-CT images in coronal orientation during 12 time points in the cardiac cycle, i.e., temporal resolution 10 ms. The spatial resolution was 0.1 mm and isotropic.

Comparison of spatial resolution in MRM and micro-CT requires that one be aware of the three- dimensional structure of the heart. The cross-sectional images in both Figures 7 and 8 are extracted from a stationary plane in the scanner. As the heart contracts, it also moves into and out of that plane. The in-plane resolution for the images in Figures 7 and 8 is comparable. But the much thinner slices from the micro-CT result in much reduced volume averaging of the slice. Moreover, as seen in Figure 4, the micro-CT provides a truly 3D image at each point in the cardiac cycle. Thus, the strength of micro-CT is the higher resolution and the true 3D image. The major weakness of CT is the high radiation dose. The smaller voxels require much higher exposures than those in the clinical arena. A minimum acquisition of systole and diastole required for cardiac ejection estimation would involve 0.3 Gy, while acquisition of 10 points during the cardiac cycle for wall motion analysis results in a dose of ~1.5 Gy. This dose is significant, but is a few times under the mouse lethal dose that ranges from 5.0 to 7.6 Gy (Ford et al., 2003). Nevertheless, using such high doses can certainly have significant impact on experimental design and results.

A comparison of advantages and disadvantages for cardiac MRM versus cardiac micro-CT imaging in rodents is shown

TABLE 3.—Advantages and disadvantages of cardiac MRM versus cardiac micro-CT.

	MRM	Micro-CT
Resolution		
Temporal resolution	+	+
Spatial resolution	+	++
SNR	+	++
Contrast mechanisms		
Flow visualization	++	−
Tagging	++	−
Perfusion	++	−
Scan time	+	++
Triggering	+	++
Radiation dose	++	−

by Table 3. In vivo imaging techniques must be carefully chosen in the context of the experimental design. The imaging modalities can be differentiated by attributes such as spatial temporal and contrast resolution. But animal support issues, radiation, use of contrast agents, and cost cannot be ignored. Both MRM and micro-CT can be used to accurately characterize cardiac anatomy such as left ventricle volume and mass in transgenic mouse models. To date, the majority of the tomographic imaging studies of cardiac physiology in murine models have used MRI. The soft tissue contrast in MRI is a powerful attribute. But micro-CT with a combination of high flux X-ray tube, careful physiologic gating, and the use of blood pool contrast agents has resulted in image sets with voxels of 1×10^{-3} mm^3, roughly 10–50 times higher spatial resolution than has been seen with MRI (Nahrendorf et al., 2003; Wiesmann et al., 2003). Both MR and micro-CT "have arrived" and are being used in a wide variety of studies. The use of MR and CT in toxicology has been limited primarily by access. Further technical developments and a concerted effort to design appropriate trials for toxicology will no doubt remove any remaining barriers.

ACKNOWLEDGMENTS

Work was performed at the Duke Center for In Vivo Microscopy, an NIH/NCRR National Biomedical Technology Resource (NCRR P41 RR005959), with additional support from NCI R24 CA 092656, and NHLBI 5R01-HL055348. We thank Thomas Foo (General Electric Healthcare) for providing the clinical human MR images.

REFERENCES

Al-Shafei, A. I., Wise, R. G., Gresham, G. A., Bronns, G., Carpenter, T. A., Hall, L. D., and Huang, C. L. (2002). Non-invasive magnetic resonance imaging assessment of myocardial changes and the effects of angiotensin-converting enzyme inhibition in diabetic rats. *J Physiol* **538**, 541–53.

Badea, C., Fubara, B., Hedlund, L., and Johnson, G. (2005). 4D micro-CT of the mouse heart. *Molecular Imaging*, in press.

Badea, C., Hedlund, L. W., Wheeler, C., Mai, W., and Johnson, G. A. (2004a). Volumetric micro- CT system for in vivo microscopy, *IEEE International Symposium on Biomedical Imaging: From Nano to Macro*, April 15–18, Arlington, VA, 1377–81.

Badea, C. T., Hedlund, L. W., and Johnson, G. A. (2004b). Micro-CT with respiratory and cardiac gating. *Med Phys* **31**, 3324–29.

Barone, F. C., Coatney, R. W., Chandra, S., Sarkar, S. K., Nelson, A. H., Contino, L. C., Brooks, D. P., Campbell, W. G., Jr., Ohlstein, E. H., and Willette, R. N. (2001). Eprosartan reduces cardiac hypertrophy, protects heart and kidney, and prevents early mortality in severely hypertensive stroke-prone rats. *Cardiovasc Res* **50**, 525–37.

Berr, S., Roy, R. J., French, B. A., Yang, Z., Gilson, W., Kramer, C. M., and Epstein, F. (2005). Black blood gradient echo cine magnetic resonance imaging of the mouse heart. *Magn Reson Med* **53**, 1074–79.

Brau, A. C. S., Cofer, G. P., Hedlund, L. W., Tajik, J. K., and Johnson, G. A. (2000). Functional cardiac microscopy using projection encoding. ISMRM 8th Scientific Meeting, pp. 659.

Brau, A. C. S., Hedlund, L. W., and Johnson, G. A. (2004). Cine magnetic resonance microscopy of the rat heart using cardiorespiratory-synchronous projection reconstruction imaging. *J Magn Res Imag* **20**, 31–38.

Camici, P. G. (2003). Gated PET and ventricular volume. *J Nucl Med* **44**, 1662.

Dawson, D., Lygate, C. A., Saunders, J., Schneider, J. E., Ye, X., Hulbert, K., Noble, J. A., and Neubauer, S. (2004). Quantitative 3-dimensional echocardiography for accurate and rapid cardiac phenotype characterization in mice. *Circulation* **110**, 1632–7.

Durney, C., Ailion, D., and Cutillo, A. (1996). Susceptibility effects (tissue-induced inhomogeneous broadening) in lung magnetic resonance. In Application of Magnetic Resonance to the Study of the Lung (A. Cutillo, Ed.). Futura Publishing Company, Inc., Armonk, NY.

Ford, N. L., Thornton, M. M., and Holdsworth, D. W. (2003). Fundamental image quality limits for microcomputed tomography in small animals. *Med Phys* **30**, 2869–77.

Franco, F., Dubois, S. K., Peshock, R. M., and Shohet, R. V. (1998). Magnetic resonance imaging accurately estimates LV mass in a transgenic mouse model of cardiac hypertrophy. *Am J Physiol* **274**, H679–83.

Gewalt, S. L., Glover, G. H., Hedlund, L. W., Cofer, G. P., MacFall, J. R., and Johnson, G. A. (1993). MR microscopy of the rat lung using projection reconstruction. *Magn Reson Med* **29**, 99–106.

Glover, G., and Pelc, N. (1988). Method of reducing image artifacts due to periodic signal variances in NMR imaging. *U.S. Patent 4,663,591*.

Haacke, E. M., Brown, R. W., Thompson, M. R., and Venkatesan, R. (1999). *Magnetic resonance imaging: physical principles and sequence design*. Wiley-Liss, New York, NY.

Hedlund, L. W., and Johnson, G. A. (2002). Mechanical ventilation for imaging the small animal lung. *ILAR J* **43**, 159–74.

Hedlund, L. W., Johnson, G. A., and Mills, G. I. (1986). Magnetic resonance microscopy of the rat thorax and abdomen. *Investig Radiol* **21**, 843–46.

Hoit, B. D. (2001). New approaches to phenotypic analysis in adult mice. *J Mol Cell Cardiol* **33**, 27–35.

Hoit, B. D., and Walsh, R. A. (2001). *Cardiovascular Physiology in the Genetically Engineered Mouse*. Kluwer Academic Publishers, Norwell, MA.

Itskovich, V. V., Choudhury, R. P., Aguinaldo, J. G. S., Fallon, J. T., Omerhodzic, S., Fisher, E. A., and Fayad, Z. A. (2003). Characterization of aortic root atherosclerosis in ApoE knockout mice: high resolution in vivo and ex vivo MRM with histological correlation. *Magn Reson Med* **49**, 381–85.

James, J. F., Hewett, T. E., and Robbins, J. (1998). Cardiac physiology in transgenic mice. *Circ Res* **82**, 407–15.

Jorgensen, S. M., Demirkaya, O., and Ritman, E. L. (1998). Three-dimensional imaging of vasculature and parenchyma in intact rodent organs with X-ray micro-CT. *Am J Physiol* **275**, H1103–14.

Lazebnik, R. S., and Wilson, D. L. (2001). Newer in vivo imaging modalities. In *Cardiovascular Physiology in the Genetically Engineered Mice* (Hoit B. D., Ed.), pp. 377–96. Kluwer Academic Publishers, Norwell, MA.

Nahrendorf, M., Hiller, K. H., Hu, K., Ertl, G., Haase, A., and Bauer, W. R. (2003). Cardiac magnetic resonance imaging in small animal models of human heart failure. *Med Image Anal* **7**, 369–75.

Paulus, M. J., Gleason, S. S., Easterly, M. E., and Foltz, C. J. (2001). A review of high-resolution X-ray computed tomography and other imaging modalities for small animal research. *Lab Anim (NY)* **30**, 36–45.

Paulus, M. J., Gleason, S. S., Kennel, S. J., Hunsicker, P. R., and Johnson, D. K. (2000). High resolution X-ray computed tomography: an emerging tool for small animal cancer research. *Neoplasia* **2**, 62–70.

Ruff, J., Wiesmann, F., Hiller, K.-H., Voll, S., von Kienlin, M., Bauer, W. R., Rommel, E., Neubauer, S., and Haase, A. (1998). Magnetic resonance microimaging for noninvasive quantification of myocardial function and mass in the mouse. *Magn Res Med* **40**, 43–48.

Ruff, J., Wiesmann, F., Lanz, T., and Haase, A. (2000). Magnetic resonance imaging of coronary arteries and heart valves in a living mouse: Techniques and preliminary results. *J Magn Reson* **146**, 290–6.

Scheffler, K., and Lehnhardt, S. (2003). Principles and applications of balanced SSFP techniques. *Eur J Radiol* **13**, 2409–18.

Slawson, S. E., Roman, B. B., Williams, D. S., and Koretsky, A. P. (1998). Cardiac MRI of the normal and hypertrophied mouse heart. *Magn Res Med* **39**, 980–87.

Vera, D. R., and Mattrey, R. F. (2002). A molecular CT blood pool contrast agent. *Acad Radiol* **9**, 784–92.

Wang, G., and Vannier, M. (2001). Micro-CT scanners for biomedical applications: An overview. *Adv Imag* **16**, 18–27.

Weichert, J. P., Lee, F. T. J., Longino, M. A., Chosey, S. G., and Counsell, R. E. (1998). Lipid-Based blood pool CT imaging of the liver. *Acad Radiol* **5**, S16–19.

Wiesmann, F., Ruff, J., Hiller, K. H., Rommel, E., Haase, A., and Neubauer, S. (2000). Developmental changes of cardiac function and mass assessed with MRI in neonatal, juvenile, and adult mice. *Am J Physiol Heart Circ Physiol* **278**, H652–7.

Wiesmann, F., Szimtenings, M., Frydrychowicz, A., Illinger, R., Hunecke, A., Rommel, E., Neubauer, S., and Haase, A. (2003). High-resolution MRI with cardiac and respiratory gating allows for accurate in vivo atherosclerotic plaque visualization in the murine aortic arch. *Magn Reson Med* **50**, 69–74.

Yea, Y., Zhu, J., and Wang, G. (2004). Geometric studies on variable radius spiral cone-beam scanning. *Med Phys* **31**, 1473–80.

Zhou, R., Pickup, S., Glickson, J. D., Scott, C. H., and Ferrari, V. A. (2003). Assessment of global and regional myocardial function in the mouse using cine and tagged MRI. *Magn Reson Med* **49**, 760–64.